EasyChair Preprint

№ 4068

Paleoseismic of the Walanae Fault Zone in the South Arm of Sulawesi, Indonesia

Asri Jaya, Osamu Nishikawa and Sahabuddin Jumadil

August 23, 2020

Paleoseismic of the Walanae Fault Zone in the South Arm of Sulawesi, Indonesia

A JAYA[1,*], O NISHIKAWA[2], S JUMADIL[1]
[1] Department of Geological Engineering, Faculty of Engineering, Hasanuddin University, Makassar, Indonesia.
[2] Department of Earth Resource Science, Faculty of International Resource Science, Akita University, Akita, Japan.

E-mail: asri_jaya@geologist.com

Abstract. Walanae Fault is a major structure in the South Arm of Sulawesi region, has a seismicity history of earthquakes magnitudes range from Mw 4 to Mw 5, the structures including those that produce a low to moderate earthquakes compared to a series of major faults in Sulawesi Island. The greatest earthquake has occurred in 1997 with a magnitude of Mw 5.9, the structures in this region were reactivated after the Donggala-Palu earthquake attach Sulawesi Island in 2018. To reinforce the activity and paleoseismicity in this region we have conducted radiocarbon dating ages from two representative locations along the East Walanae fault (EWF), two samples were collected in the middle of Walanae Fault trace yielded ages of BC 3050 cal BP and 3990 cal BP from the organic rich-soil shear band, two samples were collected in the north of Walanae Fault trace shows AD 101 cal pMC and 340 cal BP from the organic-rich soil horizon. Based on the results of radiocarbon dating ages, seismicity information and morphology analysis around the Walanae Fault region, we conclude that the Walanae fault is active and must remain a concern as an earthquake source that has potential hazards in this region, especially due to between the two structural lineaments of the West Walanae Faults (WWF) and East Walanae Fault (EWF) have lowlands that present a high risk of amplification of ground motions are inhabited by a high population among other cities on Sulawesi Island.

1. Introduction

Sulawesi Island is located in a complex tectonic setting involving three large lithospheric plates: the Eurasian Plate to the west, the Pacific Plate to the east, and the Indian-Australian Plate to the south. The Neogene tectonic history of Sulawesi is characterized by a continent-continent collision that occurs between Sundaland and Australian Craton-derived blocks ([1]-[10]) resulting in the development of large-scale active strike-slip faults, and active thrust faults, and local extensions, and magmatism related to extensive lithospheric melting ([5], [11]). Several large-scale active faults occur in Sulawesi Island which has the potential as an earthquake source, such as Gorontalo fault in the northern part of Sulawesi, the Palu-Koro Fault in the central Sulawesi, the Matano and Balantak faults in the eastern arm, Lawanopo and Kolaka faults in the southeast. Thrust faulting such as North Sulawesi mega-thrust in the northern arm, Sangihe, and Batui thrusts in the eastern arm, Tolo thrust in the southeast arm, Makassar and Majene thrust in the southwest arm. Some thrusts related to subduction slabs such as

North Sulawesi thrust and Moluccas double-subduction controlled Sangihe thrust and some even meet strike-slip like the northwestern tip of Palu-Koro as shown in Figure 1.

The variety of faults in this area is associated with intense seismic activity both individual faults and within the slab and on the thrust faults [11]. Structures of Sulawesi have moderate to high slip-rates, produced a magnitude of Mw 6-8 for individual faults and Mw> 8 for thrusts within slab ([11]-[13]), MMI (Modified Mercalli Intensity) scale from V-IX based on the 500 years return period and almost all faults in the region have lowlands with a potential accumulation of sediment that has high amplification [11].

The Walanae Fault zone is also a major structure with prominent linear landform features that is traceable over 130 km through the southern arm of Sulawesi as shown in Figure 1 ([11], [14], [15], [16], [17], [18]). The Walanae Fault system comprises two parallel faults, the West Walanae Fault (WWF) and the East Walanae Fault (EWF), with a narrow topography depression in between. The two faults purportedly formed during the end of the Middle Miocene ([14]-[15]) along the eastern margin of the western mountain range and the western margin of the Bone Mountains, respectively. The WWF fault was involved in the formation of sedimentary rocks in the Sengkang Basin, although the topographic expression is still clearly visible until now confining older rocks in the western mountain range with sediment in the west Sengkang basin to the eastern (Tempe and Walanae Depression). While the EWF fault trace was across the sedimentary rocks in the east Sengkang basin so that it seems likely younger than the WWF fault ([14], [17], [18],19]).

The geomorphic trace of the EWF can be recognized as a distinct line between the Bone Mountains and the Walanae Depression, around which an intensive deformation zone is characterized by various scales of faults, folds, and related structures have developed ([17]- [18]). Therefore, the EWF is thought to have played a major role in the structural and landform developments in this region during the Neogene. The predominance of a sinistral strike-slip motion in the EWF has been assumed based on its linear topographic feature and the shear sense of its neighboring major faults, including the Masupu fault in the northern area ([1], [3], [20], [17], [18]), recently the EWF was activated as a reverse fault NE-SW-to-E-W- directed maximum compression since Piocene with a dextral component of slip with pervasive development of secondary structures in the narrow zone between Bone Mountain and Walanae Depression [18]. However, the paleoseismic and the earthquake hazard of the Walanae Fault is still limited. Meanwhile, this region has lowlands with soft sediments and is inhabited by the highest human population over Sulawesi Island.

2. Methods

To constrain the age of the paleoseismic of the Walanae Fault, radiocarbon dating was performed for four samples of organic matter included in the soil shear band and the organic-rich soil horizon was involved in deformation near the EWF trace. Sampling was carried out at two sites in the middle and north along the EWF fault line as described in Figure 2. The first location was exposed along with a short cliff in the Lapaddata around the Bone area which is the central area of the fault trace, the area including the alluvial fan derived from the EWF fault, location placed on the approximately one-kilometer distance to the west of the main fault as shown in Figure 3.a. Two sheared soil samples with sample numbers ST-28A and ST-28B were collected in the wall of the quarry as shown in Figure 3 and Table 1. The second location is along the Pattirosompe hill around the Sengkang area on the northern part of the EWF fault line, located in the hills across the fault line on the east side of the Sengkang anticline. This region is scarp-derived colluvium from the most recent event as characteristic earthquake model such as described by [21], the second collection of organic-rich soil samples with sample numbers SKM-02 and SKG-03 were collected in the wall of Pattirosompe quarry as shown in Figure 4.a, 4.b and 4.c, stratigraphically the position of the sample beneath of the crystalline carbonate outcrop of the Taccipi Formation. The samples have been removed weathered surfaces to prevent contamination.

The collected samples were sieved to separate root and plant debris and then treated with hydrochloric acid (>3N) wash to remove carbonate minerals from organic matter. The samples were

dated using accelerator mass spectroscopy (AMS) at Beta Analytic Inc., Miami, Florida. The radiocarbon ages measured were converted to conventional radiocarbon ages [22], calibrated by the IntCal04 calibration curve [23], calibrated by the SHCAL13 calibration curve [24]. The δ13C values are reported relative to PDB.

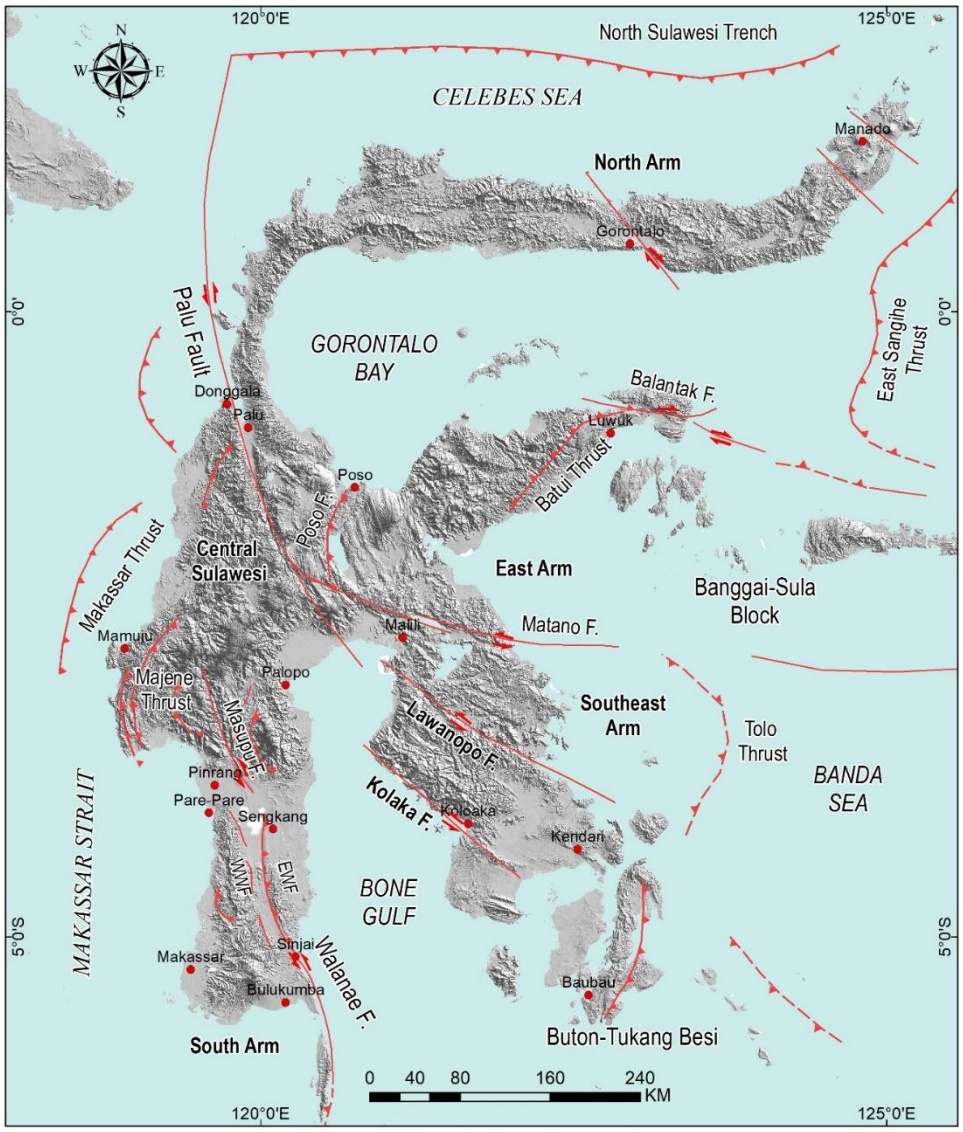

Figure 1. The topographic map and the main active fault structures of the Sulawesi region, modified after ([1], [8], [11], [13], [15], [25]).

3. Results

3.1. Geomorphological Descriptions

The East Walanae Fault can be traced over 130 km as a distinct linear feature of NNW-SSE landform trending in its southern part and N-S trending in its central and northern parts as shown in Figure 1. In the southern and central parts, the trace of the EWF is recognized along the foot of scarps that divide the areas of the Bone Mountains and the Walanae Depression. In the central part, a more continuous lineament diverges from the main EWF trace and runs parallel approximately 3 km to the east. Between these two lineaments, the land is hilly, and there are a furrowed mountain face and a narrow spacing

drainage pattern that trend slightly obliquely (up to 20°) to the EWF trace shown in Figure 2. This landform features most likely result from differential erosion of steeply dipping strata associated with folding. In its northern part, the trace of the EWF can be drawn along the east flank of a ridge of the Sengkang Anticline as shown in Figure 1 ([11], [19]). The Walanae Depression is lowland between the East and West Walanae Faults that is approximately 15 km wide. Topographic maps and cross-sections in Figure 2 show that the NNW-SSE elongating basin structure is developed on the eastern side of the depression, the floor of which is flat and gently inclined toward the center of the depression. The basin is likely aggraded by alluvial fans deposits provided via small rivers from the Bone Mountains as shown in Figure 3.a, although fan morphologies are scarcely distinct, and dissected by the channels. On the western side, the Walanae River, a main river in the depression, flows northward down cutting the low hills and forming an entrenched meander.

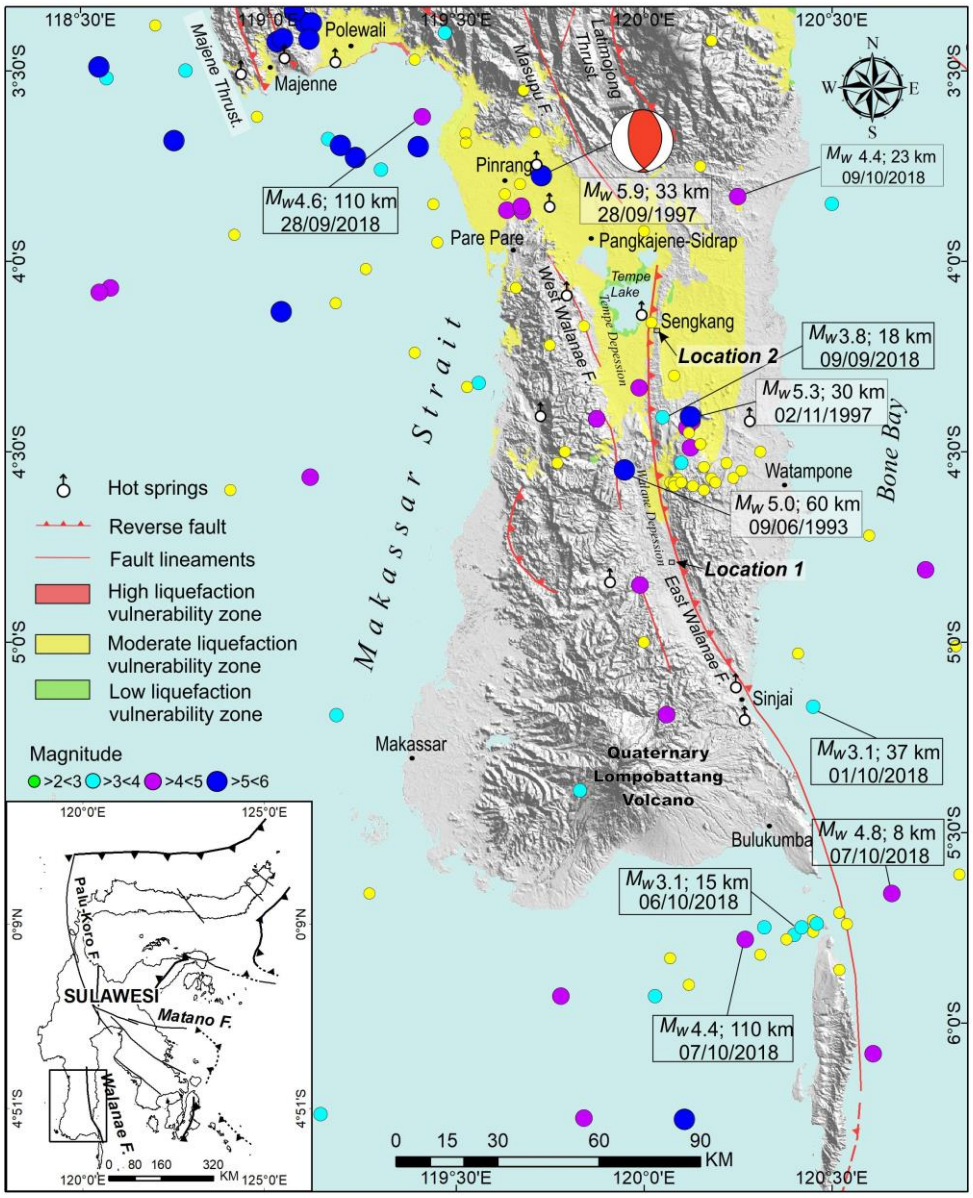

Figure 2. Structural pattern map of South Sulawesi [18]. Distribution of epicenters from low to moderate events (Mw 2–6), events from 1960-2019 around the Walanae region ([13], [26], [27]), sample locality has also shown on the map.

3.2. Seismicity of the Walanae Fault

Low to moderate magnitudes range from Mw 4-5 lead to this region rarely studied. The significant earthquake has been occurring in 1997 Mw 5.9 with 33 km depth. This event was damaged infrastructure in the Pinrang town and the nearest urban area. So far slip-rate is not known yet from GPS [13], except for information on a strain rate of 3 mm/yr or less is suggested by GPS and seismological observations for the area covering the Makassar block [28] which may include the EWF. However, the slipe-rate from geological interpretation was recorded at 0.5 mm/yr [13]. Although the magnitude is small, a series of earthquakes had occurred after a large earthquake Mw 7.5 in the northern area around the Palu region on 28 September 2018, Mw 3.1 Sinjai to the south of the EWF on 1 October 2018 and Mw 4.2 to the north of the EWF on 9 October 2018 as shown in Figure 2, respectively. Seismic hazard assessment of the Sulawesi region was indicated the Walanae Fault is classified as high intensity and moderate hazard zone at 8 scales (MMI: V – VII), based on the 500 years return period and recurrence interval 1.0 s. [11].

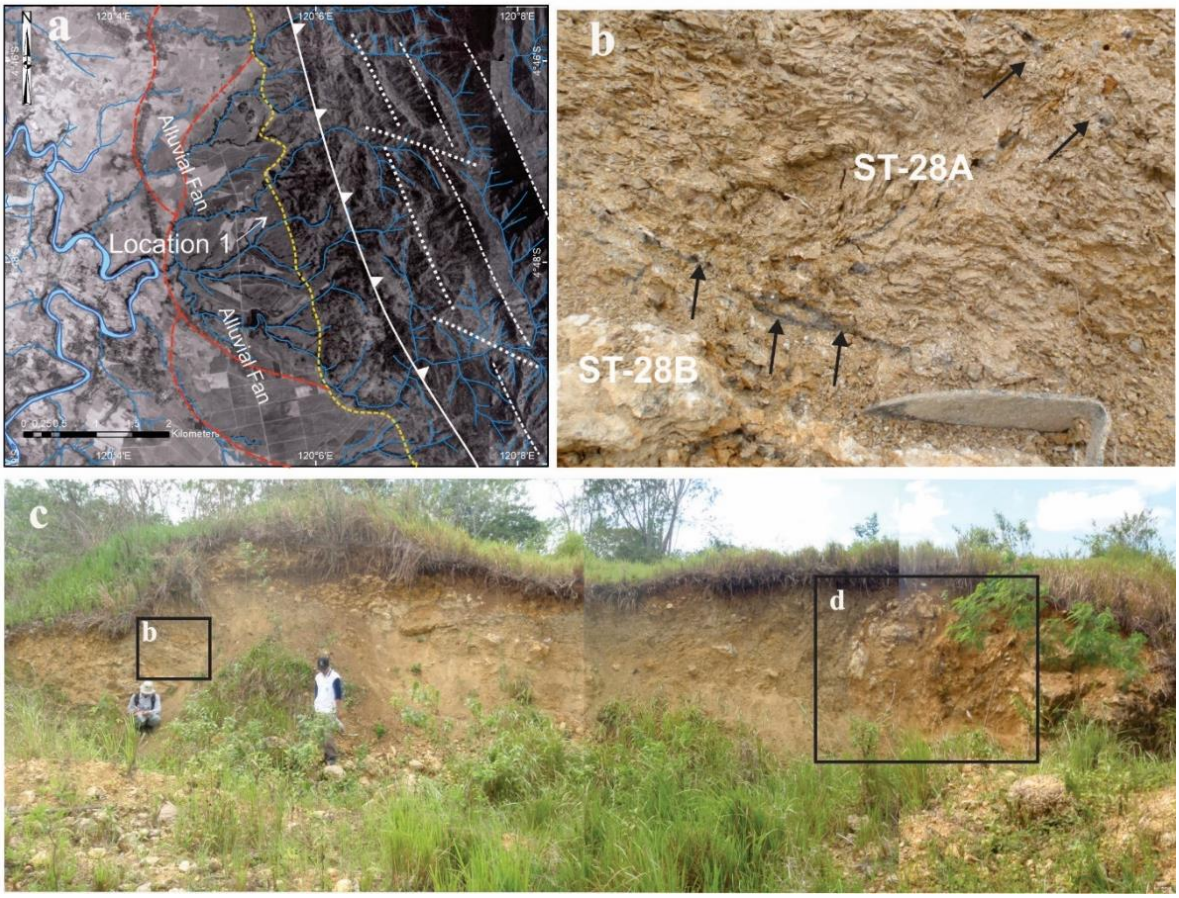

Figure 3. a) Topographic map of the center part of EWF shows morphology and structures situation around location 1 of the Bone area, the EWF fault scarp-driven alluvial fans are on the western side that shown sample locality of mine quarry. b) Close up of the occurrence of sheared soils were sampled for radiocarbon dating at the east side of the outcrop (rectangle b), dark gray soils (arrows) are intercalated among the weathered mudstone intensely sliced. c) Wall of the mining quarry of deformed strata of mudstone and limestone of the Walanae Formation in the vicinity of the EWF trace. d) The tight fold developed in the central part of the outcrop (rectangle d), where beds of mudstones are intensely sheared and limestones are fragmented.

The focal mechanism of seismic data around the Walanae Fault trace is generally related to an oblique and reverse faults, it was illustrated that the current activity of EWF is not only a strike-slip fault but also is a reverse fault, especially in the onshore or north fault EWF line. A similar indication also strongly shows by paleostress data from a combination of fault-slip and calcite twin data and evidence of sedimentary patterns suggested that the Walanae Fault was originally a strike-slip fault and now has progressively a reverse fault [18].

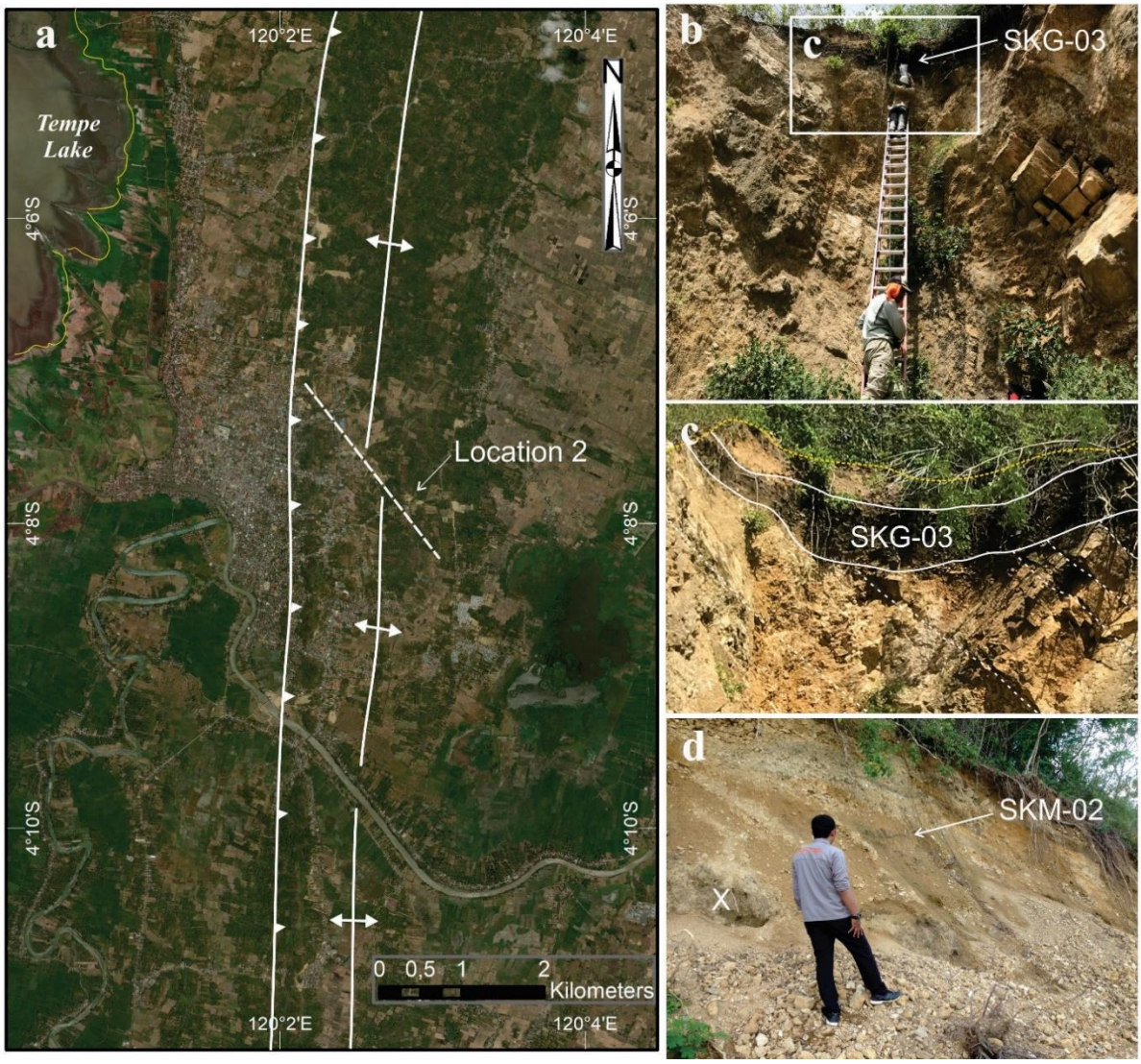

Figure 4. a) Topographic map and structures component of the center part of EWF shows morphology and structures situation around location 2 of the Sengkang area. b) Fieldwork to collect sample where contain organic rich-horizon beneath of crystalline carbonate outcrops in the wall of mining quarry in the location 2 of Sengkang area (Pattirosompe hill). c) Close up of the occurrence of sheared soils were sampled for radiocarbon dating of SKG-03 (rectangle b). d) Site of SKM-02 soil sampling (arrow), "X" marking is the continuity of the horizon of SKG-03 which field strata have a stratigraphic order than SKM-02.

3.3. Radiocarbon Dating $\delta^{13}C$ values

Sample from the Bone area as shown in Figures 2 and 3, the samples used for radiocarbon dating were soils intercalated in the shear fractures formed in the weathered mudstone which is intensely sliced by

flexural slip folding most likely associated with the activity of the EWF as shown in Figure 3.d. The soils include dark-brown organic matter. Samples ST-28A and ST-28B, which come from 50 cm and 30 cm beneath the surface, respectively, yielded ages of 3050 cal BP and 3990 cal BP shown I Table 1. These radiocarbon ages are consistent with the stratigraphic order. The $\delta^{13}C$ (PDB) values of the date soil samples are also shown in Table 1. Both samples show similar and significantly negative values, –18.4‰ for ST.28A and –19.6‰ for ST-28B as shown in Table 1, which are plausible for soils of grassland.

Two samples of organic-rich soil horizon underneath of crystalline limestone at the same location of Pattirosempe hill in the Sengkang area as shown in Figures 2 and 4, not indirectly strata order but still correlated in the field are used for radiocarbon dating as shown in Figure 4.a and 4.c. Soil samples came from a colluvial wedge of the east limb of the Sengkang anticline, SKG-03 was collected from 60 cm beneath the surface, while SKM-02 was collected from 100 cm from the surface, stratigraphically SKG-03 is older than SKM-02 as shown in Figure 4.a, 4.b, and 4.c. The dating results also consistently with stratigraphic order as shown in Table 1, SKM-02 yielded an age of 101 cal pMC and SKG-03 yielded an age of 340 cal BP. The ~200-year difference represents two different earthquake events. The δ13C (PDB) values of the date soil samples are also shown in Table 1. Both samples show similar and significantly negative values, –24.6 ‰ for SKM-02, –19.6 ‰ for SKG-03 shown in Table 1, which are plausible also for soils of grassland.

Compared to location 1 in the Bone area, the age at location 2 in the Sengkang area is the most recent faulting event at this site. The range of ~2700 to ~2900 years gap of both locations shown in Table 1 is likely due to the sample at location 1 is a fissure and crack of the alluvial fan and far from the main fault, approximately ± 1 km from the EWF fault trace as shown in Figure 3.a, whereas in location 2 is a deposition wedge directly from Walanae Fault trace. All organic soil data has shown a well paleoseismic record around the region. To assess seismic risk in the future, we still need to add more information to the completed study in this area.

Table 1. Radiocarbon ages dating of soil samples.

Sample number	Lab sample number [a]	Measured radiocarbon age	$\delta^{13}C$(‰)	Conventional radiocarbon age (BP) [b]	Calibrated age 2σ
ST-28A	Beta-286412	2940 ± 40	-18,4	3050 ± 40	Cal BC 1410-1210, Cal BP 3360-3160 (95% probably) [c]
ST-28B	Beta-286413	3900 ± 40	-19,6	3990 ± 40	Cal BC 2580-2460, Cal BP 3530-4410 (95% probably) [c]
SKM-02	Beta-437032	101 ± 40	-24.6	101 ± 50	pMC = percent modern carbon
SKG-03	Beta-479286	340 ± 30	-19.6	340 ± 30	Cal AD 1496 - 1650, 454 - 300 cal BP (95.4% probably) [d]

[a] Processing and measurement of samples were carryout at Beta Analytic Inc. Miami, Florida.
[b] Conventional ^{14}C ages were calculated according to [22].
[c] Calibration of radiocarbon age to calendar years was performed using "IntCal04" (calibration issue of radiocarbon, volume 46, 2004).
[d] Calibration of radiocarbon age to calendar years was performed using "SHCAL13" (calibration issue of radiocarbon, volume 55, 2013).

4. Discussion

4.1. Paleoseismic of the Walanae Fault

Although no obvious tectonic landform has been found and current seismicity around the EWF seems relatively low compared to Central and North Sulawesi ([28]-[31]), Late Quaternary deformation associated with the EWF activity is confirmed by our radiocarbon dating, which yielded approximately BC ~3000 to ~4000 and AD ~100 to ~300 years as shown in Table 1. Based on the seismotectonic study, the present-day deformation and stress field in South Sulawesi are characterized by a compressional regime with ESE-WNW (N99°E)-trending σ1 ([18], [30], [32]) showed the dominance of reverse faulting in South Sulawesi. Therefore, it can be accepted that the stress states of E-W to NE-SW general compression have continued consistently since the Late Miocene.

There is currently no data available on average rupture length and slip-rate for the Walanae Fault, if the empirical relationships are applied by [33], when the entire fault (~130 km) is ruptured at once, by applying modern magnitude earthquakes currently applied averaging Mw 5-6 did not rupture the surface in this areas, with such a length it is likely to produce Mw 6-7. This magnitude seems to agree with rupture scenarios of the events for the future.

4.2. Earthquake Hazard of Walanae Fault

Individually earthquake hazards along the Walane fault trace appear to be high [11], with lowlands along with the Walanae Depression and Tempe Depression created by the fault leading to high amplification (site classes D and E) of ground motions [11]. Part of the depression area was classified as a moderate liquefaction vulnerability zone [34]. Earthquake history has been recorded from 1993 to 1997 in the northern part of the Walanae valley with an average magnitude of Mw 4-5 and an earthquake in 1997 with a magnitude of Mw 5.9 on the same side as shown in Figure 2. The earthquake reportedly swallowed 16 people died and hundreds of buildings were destroyed (local government and online news information). These high potential earthquake hazards and paleoseismic were correlated well with the historical earthquake damage in the region, except for the damaging 29/12/1828 earthquake in Bulukumba with MMI scale of VIII-IX, on the south coast of South Sulawesi and even the tsunami around Makassar in 1820 with MMI scale VII [26]. However, the earthquake that occurred ± 200 years ago was not equipped with coordinate information and the possibility of having been caused by either the Walanae Fault or an unmapped offshore extension of this structure to the SE [11].

Although in general, this region has a few historical earthquakes recorded much lower than over the Island. Research and documentation of earthquake hazard data in this region should be continued since the region has presented several small towns inhabited by significant populations, an average of 50,000 inhabitants in the Walanae valley from north to south such as Pinrang, Pangkajene-Sidrap, Sengkang, Sinjai and Bulukumba, respectively. It can also be considered that the major faults in the middle part of Sulawesi are quite large in intensity and magnitude so that if there is ground shaking by a large earthquake in the area it possibly influenced the Walanae region, such as the Palu earthquake of 2018. Another consideration that physiographically this region is the boundary between the Walanae valley and the northern highlands of the Majene and Masupu faults, it can be influenced by these thrusts which have high earthquake intensity and seismicity. As was the case when a major earthquake occurs in the Central Sulawesi in 2018, this region also showed significant activity.

5. Conclusion

Novel insights derived from our field investigations, radiocarbon dating, paleoseismic, and earthquake hazard analysis of Walanae Fault in the South Arm of Sulawesi can be summarized in the following points:

- The Late Quaternary radiocarbon ages BC 3050 cal BP and 3990 cal BP of sheared soils indicated that the deformation is still active around the Walanae Fault.
- The most recent two radiocarbons dating from organic-rich soils of AD pMC cal BP and 340 cal BP were collected from scarp-derived colluvium of main faults confirmed paleoseismic from east Walanae fault activity.

- Inferred significant recent earthquakes of 1997 which occurred around the Walanae Depression showed that both of the Walanae Fault trace and the lowlands have a high potential earthquake hazard for the future.
- Inferred the Walanae Fault is an active fault that has been proven by the activity of this fault which has been demonstrated in the aftermath of a major earthquake in the central part of Sulawesi in 2018.

Acknowledgments
This research was funded by International Research Collaboration (PKLN 2018) and Fundamental Research (PDU 2020) of Hasanuddin University. We express gratitude and appreciation to the Ministry of Education and Culture of Indonesia and Hasanuddin University for providing a research grant. We thank the reviewer for helpful comments and advice. We also thank Arman Makkaraka and the students of Hasanuddin University for supporting us during the field survey.

References

[1] Hamilton W 1979 *US Geological Survey Professional Paper* **1078**
[2] Yuwono YS, Maury R and Soeria-Atmadja R Bellon H 1988 *Geologi Indonesia Jakarta* **13** 32–48
[3] Coffield DQ, Bergman SC, Carrard RA, Guritno N, Robinson NM and Talbot J 1993 *Proceedings of the Indonesian Petroleum Association* **22** 679–706
[4] Priadi B, Polvé M, Maury RG, Bellon H, Soeria-Atmadja R, Joron JL and Cotton J 1994 *Journal of Southeast Asian Earth Sciences* **9** 81–93
[5] Bergman SC, Coffield DQ, Talbot JP and Garrard RJ 1996 *Tectonic Evolution of SE Asia* vol 106, ed Hall R and Blundell D J (London: The Geological Society Special Publications) pp 391–430
[6] Polvé M, Maury RC, Bellon H, Rangin C, Priadi B, Yuwono S, Joron JL and Soeria- Atmadja R *Tectonophysics* **272** 69–92
[7] Elburg M and Foden J 1999 *Geochimica et Cosmochimica Acta* **63** 1155–72
[8] Hall R and Wilson MEJ 2000 *Journal of Asian Earth Sciences* **18** 781–808
[9] Hall R 2002 *Journal of Asian Earth Sciences* **20** 235–431
[10] Jaya A, Nishikawa O and Hayasaka Y 2017 *Lithos* **291-293** 96–110
[11] Cipta A, Robiana R, Griffin JD, Horspool N, Hidayati S, and Cummings PR 2017 *Geohazards in Indonesia: earth science for disaster risk reduction* vol 441, ed Cummins PR and Meilano I (London: The Geological Society Special Publications) pp 133–152
[12] Irsyam M, Sengara IW, Asrurifa M, Ridwan M, Aldimar S, Widiyantoro S, Triyoso W, Natawijaya DH, Kertapati E, Meilano I and Suhardjono 2010 *Development of Seismic Hazard Maps of Indonesia for Revision of Seismic Hazard Map* SNI 03-1726-2002
[13] National Center for Earthquake Studies *(PuSGeN)* 2017 *Seismic Source and Hazard Map of Indonesia*
[14] Van Leeuwen T 1981 *The Geology and Tectonics of Eastern Indonesia* vol 2, ed Barber A and Wiryosujono S (London: The Geological Society Special Publications) pp 277–304
[15] Sukamto R 1975 *Regional Conference on the Geology and Mineral Resources of SE Asia Jakarta* 1–25.
[16] Berry RF and Grady AE 1987 *Journal of Structural Geology* **9** 563–571
[17] Van Leeuwen TM, Susant ES, Maryanto S, Hadiwisastra S, Sudijono and Muharjo 2010 *Journal of Asian Earth Sciences* **38** 233-254
[18] Jaya A and Nishikawa O 2013 *Journal of Structural Geology* **55** 34-49
[19] Grainge AM and Davies KG 1985 *Marine and Petroleum Geology* **2** 142–155
[20] Guritno Coffield DQ Cook RA 1996 *Proceedings of the Indonesian Petroleum Association* **25** 253–266
[21] Schwartz DP and Coppersmith KJ 1984 *J. Geophys Res. Solid Earth* **89** 5681–98

[22] Stuiver M and Polach HA 1977 *Radiocarbon* **19** 1029-58
[23] Reimer PJ, Bailli MGL, Bard E, Bayliss A, Beck JW, Bertand CJ, Blackwell PG, Buck C, Burr GS, Cutler KB, Damon PE, Edwards RL, Fairbanks RG, Friedrich M, Guilderson TP, Hogg AG, Hughen KA, Kromer B, McCormac Manning S Ramsey CB, Reimer R, Remmele Southo JR, Stuiver M, Talamo S, Taylor FW, van der Plicht J and Weyhenmeyer CE 2004 *Radiocarbon* **46** 1029-1058
[24] Hogg AG, Hua Q, Blackwell PG, Niu M, Buck CE, Guilderson TP, Heaton TJ, Palmer JG, Reimer PJ, Reimer RW, Turney CSM and Zimmerman SHR 2013 *Radiocarbon* **55** 1889–1903
[25] Watkinson IM 2011 The SE Asian Gateway: *History and Tectonics of the Australia–Asia Collision* vol 355, ed Hall R, Cottam MA and Wilson MEJ (Geological Society of London Special Publications) pp 157-176
[26] Supartoyo and Surono 2008 Catalog of Indonesian Destructive Earthquake the Year 1629–2007 *Geological Agency of Indonesia*
[27] Meteorological, Climatological and Geophysical Agency of Indonesia (BMKG) https://www.bmkg.go.id/?lang=EN
[28] Socquet A, Vigny C, Chamot-Rooke Simons W, Rangin C and Ambrosius B 2006 *J. Geophys Res.* **111** 1–15
[29] Bellier O, Sebrier M, Seward D, Beaudouin T, Villeneuve M and Putranto E 2006 *Tectonophysics* **413** 201–220
[30] Tanioka Y and Yudhicara 2008 *Jurnal Geoaplika* **3** 71-80
[31] Jaya A, Nishikawa O and Jumadil S 2019 *Earth Planets and Space* **71** 1-13
[32] Beaudouin TH, Bellier O and Sebrier M 2003 *Bulletin de la Société géologique de France* **174** 305-317
[33] Wells DL and Coppersmith KJ 1994 *Bull. Seismol. Soc. Am.* **84** 974–1002
[34] Geological Agency of Indonesia 2019 *Ministry of Energy and Mineral Resources of Indonesia*-Center *of Groundwater Resources and Environmental Geology*